Chapter 2: Global Oceans

Joel M. Levy, Editor

Translated by:

Overview

Joel M. Levy
NOAA/OAR Climate Program Office, Silver Spring, Maryland

As the global ocean observing system matures and climatologies of essential climate variables grow more robust, observations of anomalous departures continue to shed light on the evolving behavior of the coupled ocean-atmosphere system. The year 2008 was characterized by the following findings:

- The global mean SST in 2008 was slightly cooler than that in 2007, largely due to the cooling in the central tropical Pacific, the Arctic Ocean and the regions extending from Gulf of Alaska to the west coast of North America. The yearly mean SST anomaly in 2008 was dominated by a negative Pacific Decadal Oscillation pattern (PDO). The yearly mean PDO index in 2008 was the lowest since 1971.

- Global integrals of upper ocean heat content for the last several years have reached values consistently higher than for all prior times in the record, demonstrating the dominant role of the oceans in the Earth's heat budget. 2008 basin-scale upper ocean heat content patterns are consistent with current phasing of familiar climate indices such as ENSO.

- The basin averaged latent and sensible heat fluxes in 2008 decreased slightly from 2007, continuing the broad downward trend that started in 1999. There seems to be a tendency toward reversing the upward trend that had dominated the decades of the 1980s and 1990s. Changes in latent and sensible heat fluxes in the Pacific responded to the SST anomalies of the cool PDO phase, with enhanced heat loss over positive SST anomalies, and reduced heat loss over negative SST anomalies. By contrast, the ocean heat fluxes in the Atlantic Ocean were an important forcing for SST variability: SST increased (decreased) as a result of reduced (enhanced) heat loss at the sea surface.

- Tropical Cyclone Heat Potential values in the north central Gulf of Mexico were lower in August 2008 than in August 2005.

- Outside the tropics, the anomalously salty surface salinity values in climatologically drier locations and anomalously fresh values in rainier locations observed in recent years generally

persist in 2008, suggesting an increase in the hydrological cycle, consistent with climate model predictions for global warming scenarios. Within the tropics, 2008 sea surface salinity anomalies can be largely related to recent La Niña conditions.

- Eastward surface current anomalies in the tropical Pacific Ocean in early 2008 played a major role in adjusting the basin from strong La Niña conditions to ENSO-neutral conditions by July-August. Long-term trends in geostrophic eddy kinetic energy continue to indicate interannual to decadal shifts in major current systems such as the Gulf Stream and the Brazil-Malvinas confluence.

- Direct observations of the strength of the meridional overturning circulation show substantial variability on short time scales with some evolving evidence of a pronounced seasonal variation. Indirect observations from subsurface water properties suggest a recent strengthening of deep-water formation in the Labrador Sea and a decrease in deep water transports from the Antarctic that is both warmer and fresher than in the past.

- The La Nina event of 2007-08 affected not only regional sea level anomalies but global mean sea level (GMSL) as well. GMSL has been persistently low during the La Nina event relative to a linear trend of approximately 3.3 mm yr^{-1}. The correspondence between GMSL and the Multivariate ENSO Index highlights the strong influence of ENSO variability on global sea level. Once this interannual variability is accounted for, the inferred rate of GMSL change remains remarkably constant.

- The global mean air-sea CO2 flux for the period 1983 to 2007, including the El Niño, Southern Oscillation (ENSO) effects, gives an average uptake of 1.74 Pg-C yr^{-1}. The global mean CO2 uptake for 2007 is estimated to be 1.67 Pg-C, about 0.07 Pg-C lower than the long-term average making it the third largest anomaly determined with this method since 1983. Unlike long term findings, the North Atlantic has not had the largest increase in anthropogenic carbon storage over the last decade. The rate of carbon inventory increases in the eastern Indian Ocean was significantly higher between 1995 and 2008 than it was between 1978 and1995.

- Global phytoplankton chlorophyll concentrations were slightly elevated in 2008 relative to 2007, but regional changes were substantial (ranging to about 50%) and followed long-term patterns of net decreases in chlorophyll with increasing sea surface temperature.

Sea Surface Temperatures in 2008

Yan Xue[1] and Richard W. Reynolds[2]

[1] NOAA/NWS, Climate Prediction Center, National Centers for Environmental Prediction
Camp Springs, MD
[2] NOAA/NESDIS, National Climatic Data Center, Asheville, NC

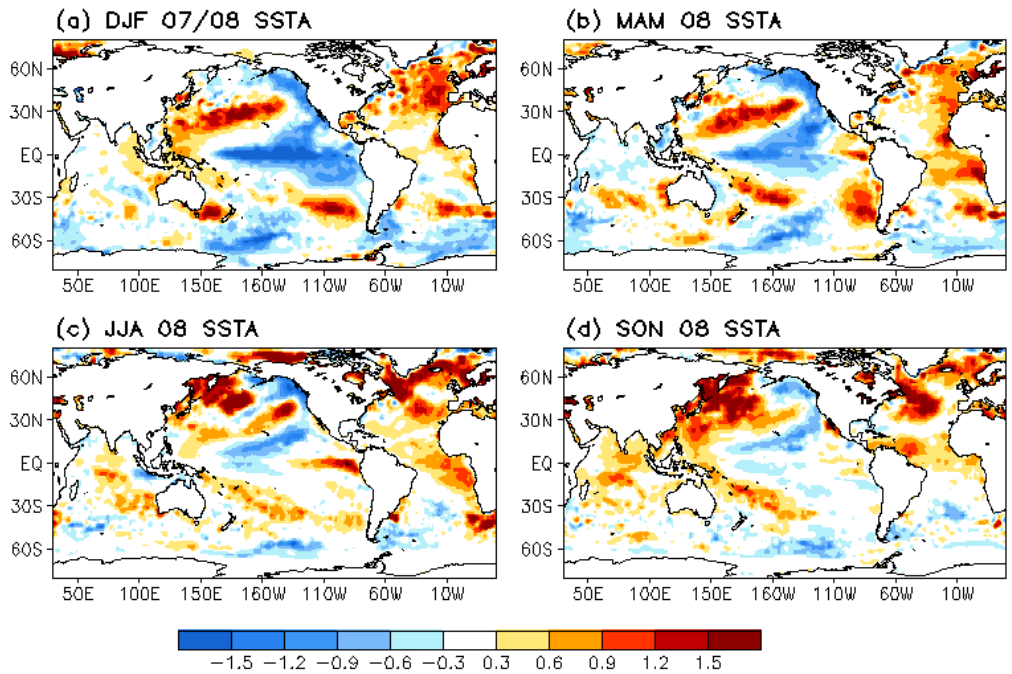

Fig. 3.1. Seasonal mean SST anomalies for (a) December 2007 to February 2008, (b) March to May 2008, (c) June to August 2008 and (d) September to November 2008. SSTs are the monthly fields interpolated from the weekly 1° Optimum Interpolation (OI) analyses of Reynolds et al. (2002). All anomalies are defined as departures from the 1971-2000 climatology (Xue et al., 2003).

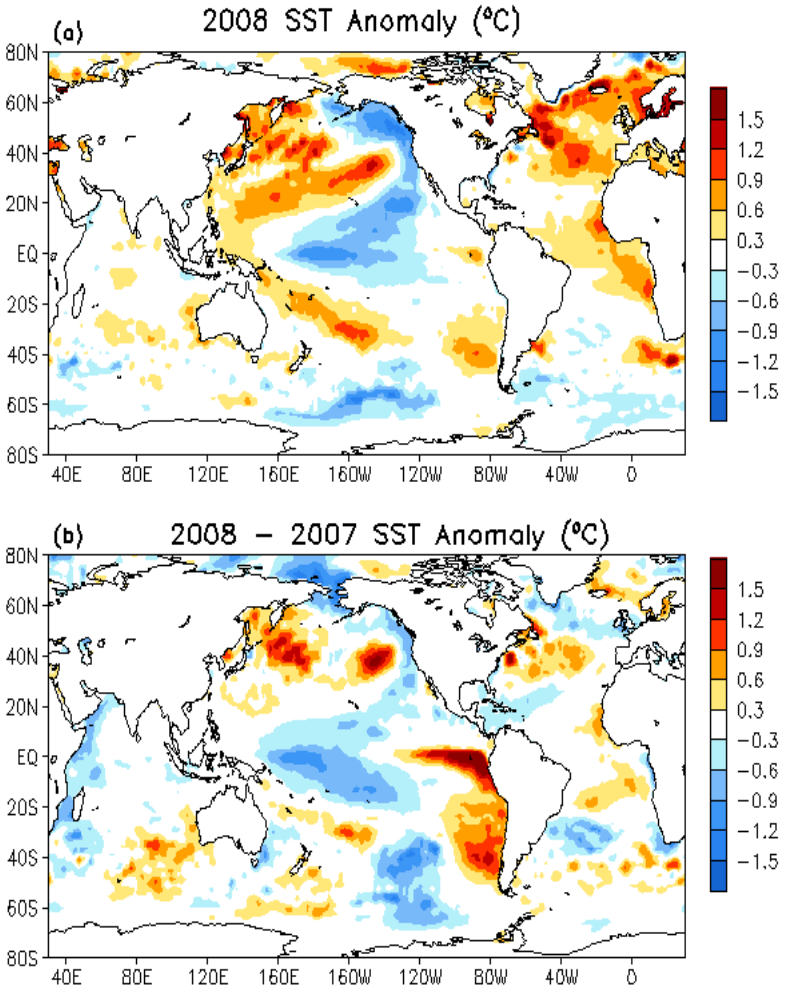

Fig. 3.2. (a) Yearly mean SST anomalies in 2008 and (b) SSTA differences between 2008 and 2007. SSTs are the monthly fields interpolated from the weekly 1° Optimum Interpolation (OI) analyses of Reynolds et al. (2002). All anomalies are defined as departures from the 1971-2000 climatology (Xue et al., 2003).

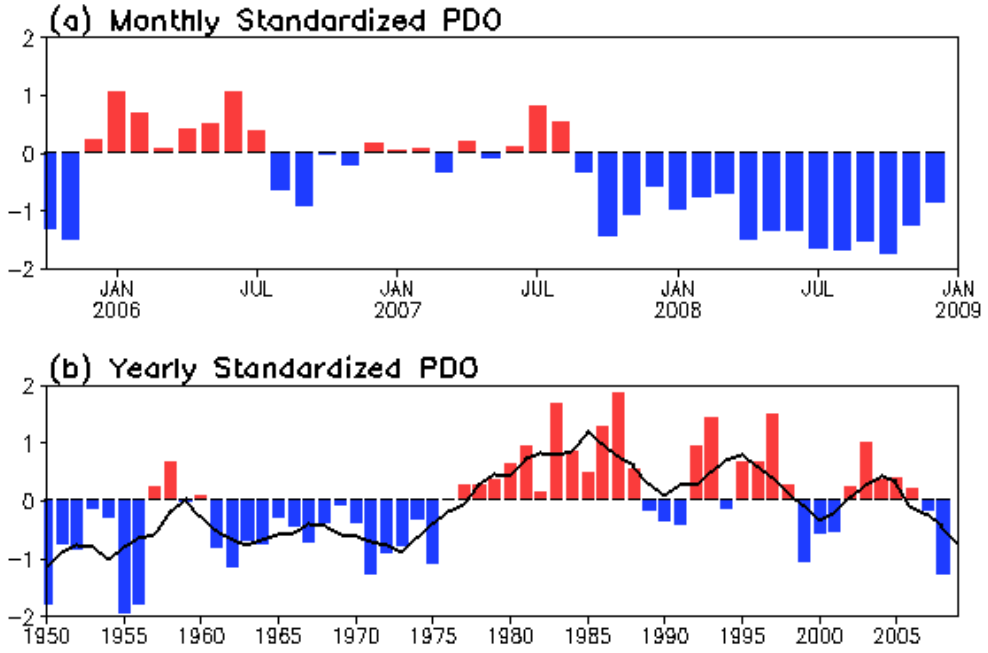

Fig. 3.3 (a) Monthly standardized Pacific Decadal Oscillation (PDO) index (bar) in the past four years and (b) yearly mean of the monthly PDO index (bar) overlapped with the five-year running mean of the index (black line) in 1950-2008. The PDO index was downloaded from University of Washington at http://jisao.washington.edu/pdo.

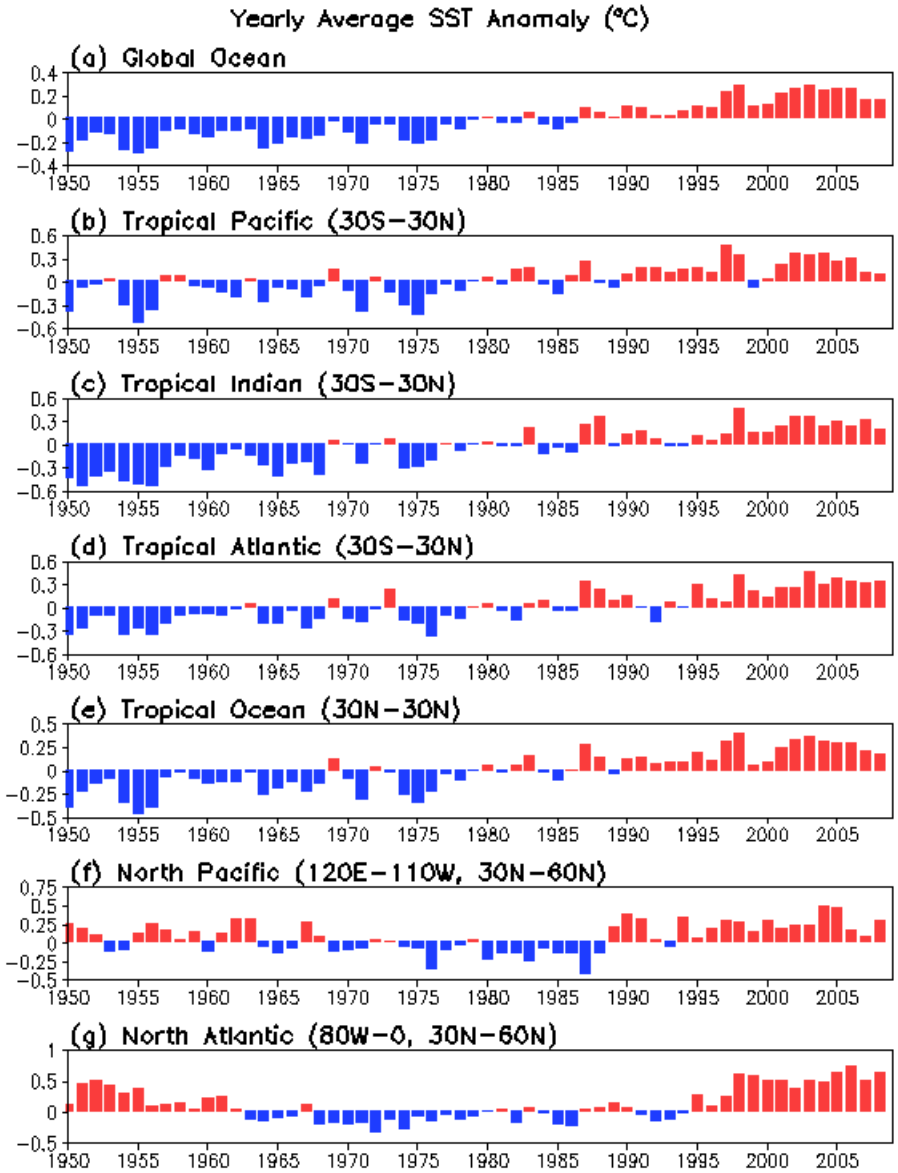

Fig. 3.4 Yearly mean SST anomalies averaged in (a) the global ocean, (b) tropical Pacific Ocean, (c) tropical Indian Ocean, (d) tropical Atlantic Ocean, (e) all three tropical Oceans, (f) North Pacific and (g) North Atlantic in 1950-2008. SSTs are the Extended Reconstructed Sea Surface Temperature version 3b (ERSST v.3b) of Smith et al. (2008). All anomalies are defined as departures from the 1971-2000 climatology (Xue et al., 2003).

Ocean Heat Content

Gregory C. Johnson[1], John M. Lyman[1,2], Joshua K. Willis[3], Sydney Levitus[4], Tim Boyer[4], John Antonov[4]. Claudia Schmid[5], and Gustavo J. Goni[5]

[1]NOAA/OAR Pacific Marine Environmental Laboratory, Seattle, WA
[2]JIMAR, University of Hawaii, Honolulu, HI
[3]NASA/Jet Propulsion Laboratory, Pasadena, CA
[4]NOAA/NESDIS National Ocean Data Center, Silver Spring, MD
[5]NOAA/OAR Atlantic Oceanographic and Meteorological Laboratory, Miami, FL

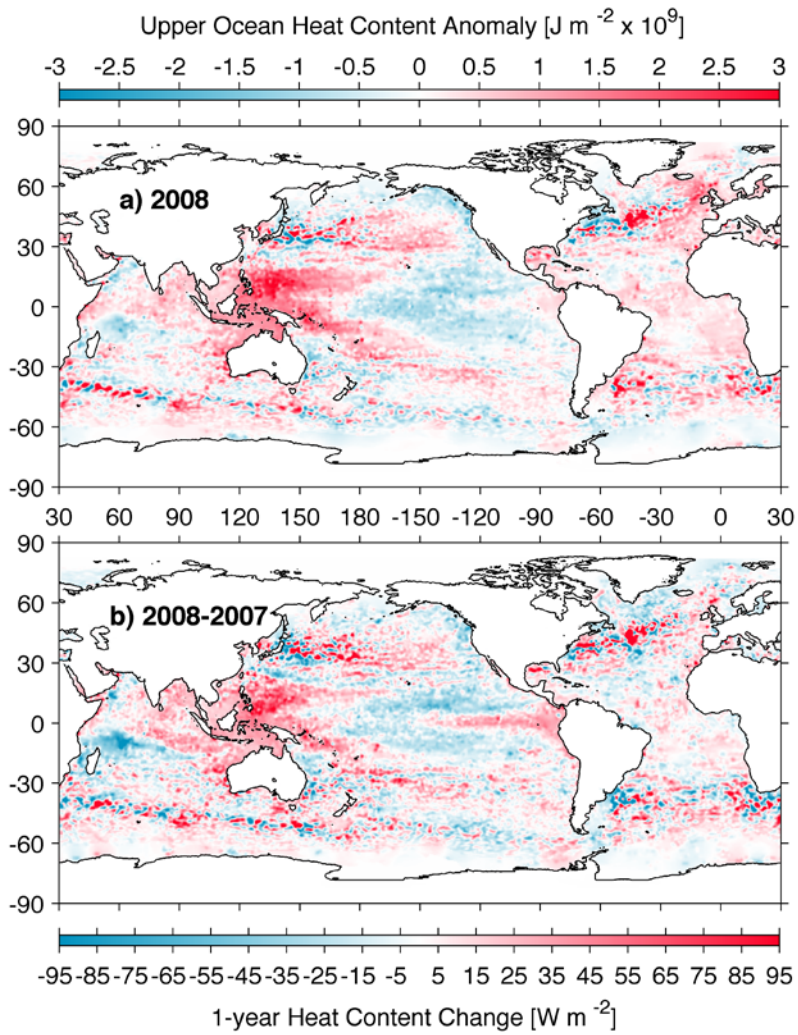

Fig. 3.5 (a) Combined satellite altimeter and in situ ocean temperature data estimate of upper (0 – 750 m) ocean heat content anomaly OHCA (10^9 J m^{-2}) for 2008 analyzed following Willis et al. (2004), but relative to a 1993 – 2008 baseline. (b) The difference of 2008 and 2007 combined estimates of OHCA expressed as a local surface heat flux equivalent (W m^{-2}). For panel

comparisons, note that 95 W m^{-2} applied over one year results in a 3×10^9 J m^{-2} change of OHCA.

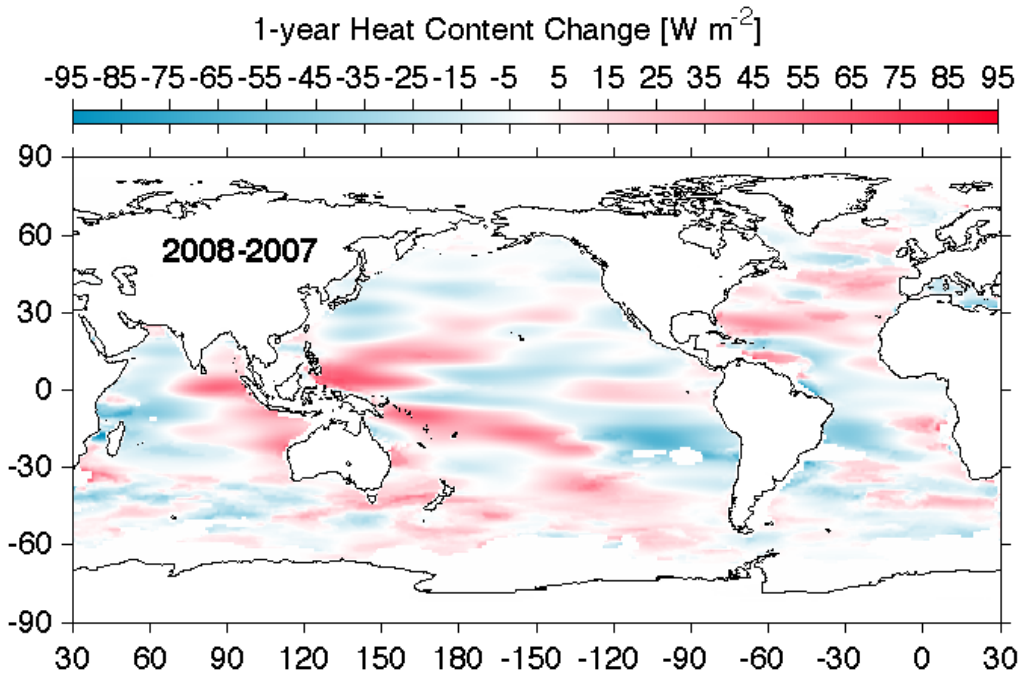

Fig. 3.6. Change of ocean mixed layer heat content estimated following Schmid (2005) expressed as a surface heat flux equivalent (W m^{-2}). The map is based on subtraction of a yearly mean of ocean mixed layer content for calendar year 2008 from that for calendar year 2007.

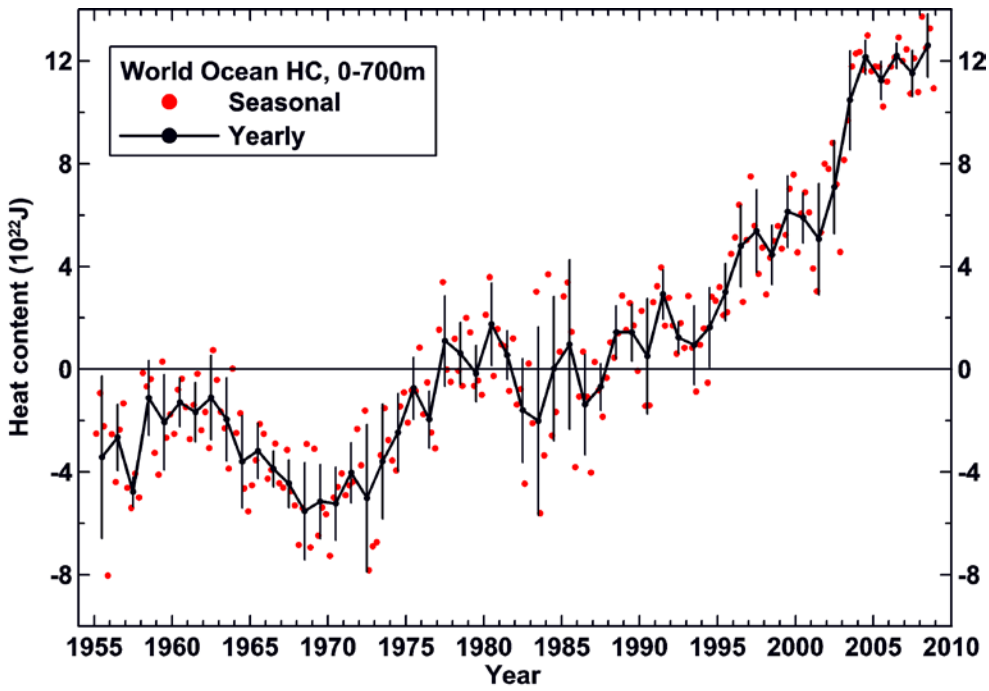

Fig. 3.7. Time series of quarterly (red dots) and annual average (black line) global integrals of in situ estimates of upper OHCA (10^{22} J) for the 0-700 m layer from 1955–2008, following Levitus et al. (2009). Error bars for the annual values are one standard deviation of the four quarterly estimates in each year. Additional error sources include sampling errors (Lyman and Johnson 2008) and remaining uncorrected instrument biases (Levitus et al. 2009).

Global Ocean Heat Fluxes

Lisan Yu and Robert A. Weller

Woods Hole Oceanographic Institution, Woods Hole, MA

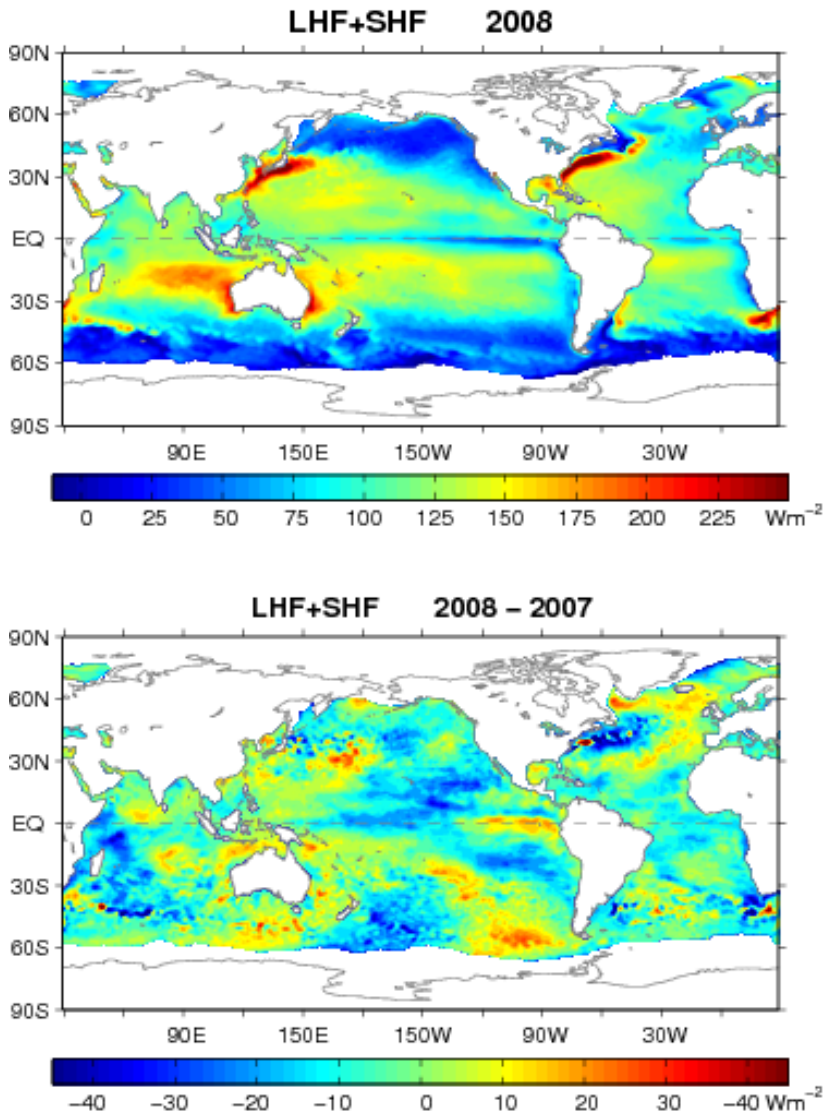

Fig. 3.8. (a) Upper panel: Annual mean latent plus sensible heat fluxes in 2008. The sign is defined as upward (downward) positive (negative). (b) Bottom panel: Differences between the 2008 and 2007 annual mean latent plus sensible heat fluxes.

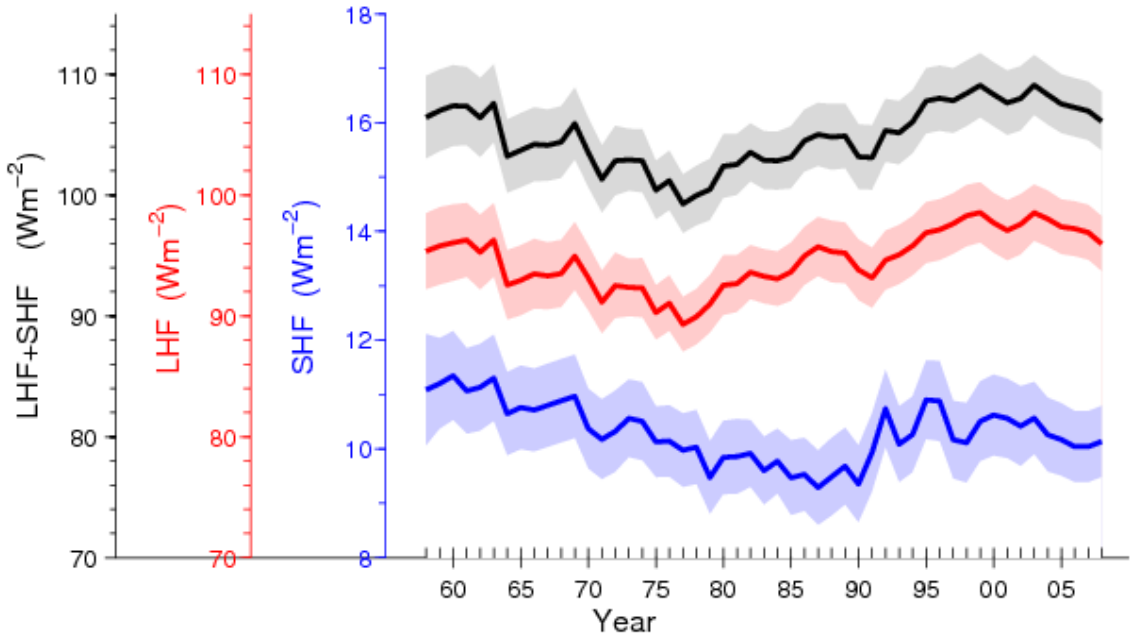

Fig. 3.9. Year-to-year variations of global averaged annual mean latent plus sensible heat flux (blue line), latent heat flux (red line), and sensible heat flux (black line). The shaded areas indicate the upper and lower limits at the 90% confidence level.

Tropical Cyclone Heat Potential

Gustavo J. Goni[1] and John A. Knaff[2]

[1] NOAA/OAR Atlantic Oceanographic and Meteorological Laboratory, Physical Oceanography Division, Miami, FL
[2] NOAA/NWS Regional and Mesoscale Meteorology Branch, Fort Collins, CO

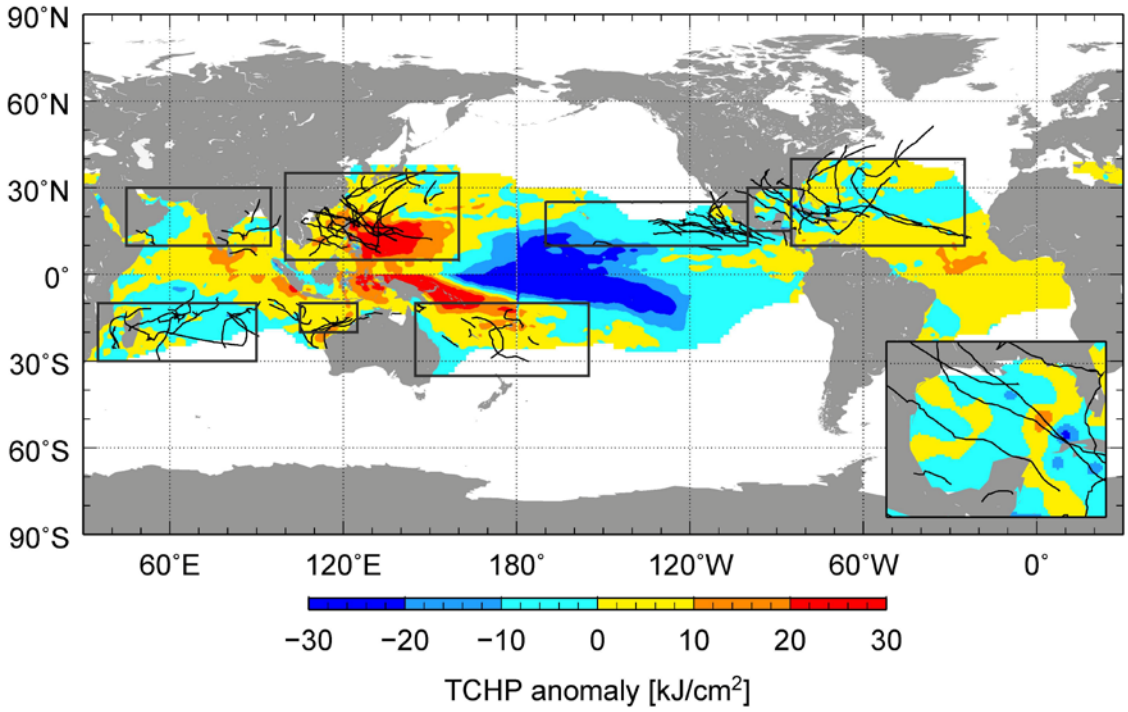

Fig. 3.10. Global anomalies of TCHP corresponding to 2008 computed as described in the text. The boxes indicate the seven regions where TCs occur: from left to right, Southwest Indian, North Indian, West Pacific, Southeast Indian, South Pacific, East Pacific, and North Atlantic (shown as Gulf of Mexico and tropical Atlantic separately). The black lines indicate the trajectories of all tropical cyclones category 1 and above during November 2007-December 2008 in the Southern Hemisphere and January-December 2008 in the Northern Hemisphere. The Gulf of Mexico conditions during June-November 2008 are shown in detail in the insert shown in the lower right corner.

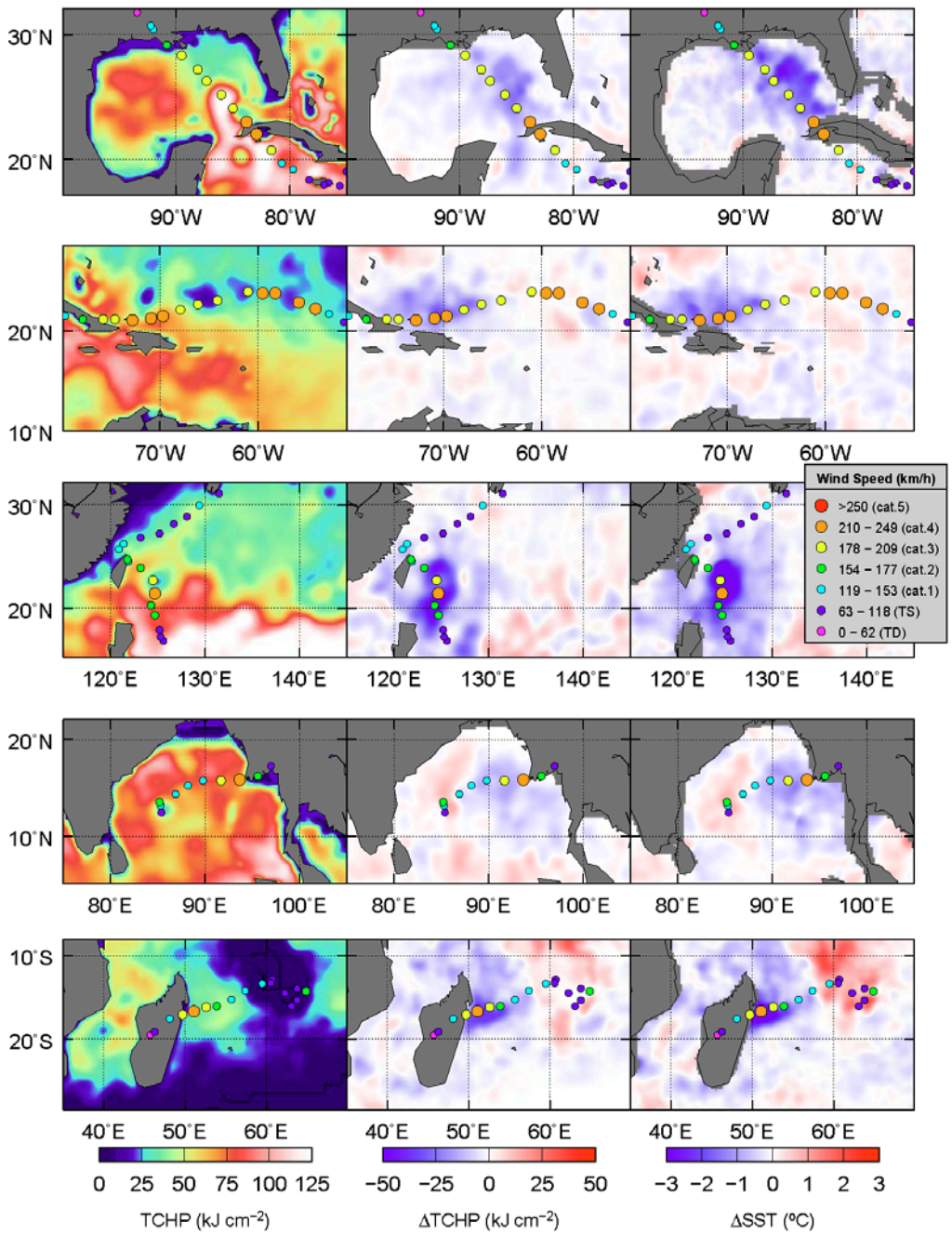
30°N
20°N
90°W
80°W
20°N
10°N
70°W
60°W
30°N
20°N
120°E
130°E
140°E
20°N
10°N
80°E
90°E
100°E
10°S
20°S
40°E
50°E
60°E
Wind Speed (km/h)
>250 (cat.5)
210 – 249 (cat.4)
178 – 209 (cat.3)
154 – 177 (cat.2)
119 – 153 (cat.1)
63 – 118 (TS)
0 – 62 (TD)
0 25 50 75 100 125
TCHP (kJ cm⁻²)
−50 −25 0 25 50
ΔTCHP (kJ cm⁻²)
−3 −2 −1 0 1 2 3
ΔSST (ºC)

Fig. 3.11. (left) Tropical cyclone heat potential, and surface cooling given by the difference between post and pre storm values of (center) tropical cyclone heat potential and (right) sea surface temperature, for (from top to bottom) Hurricane Gustav, Hurricane Ike, Typhoon Sinlaku, Tropical Cyclone Nargis, and Tropical Cyclone Ivan.

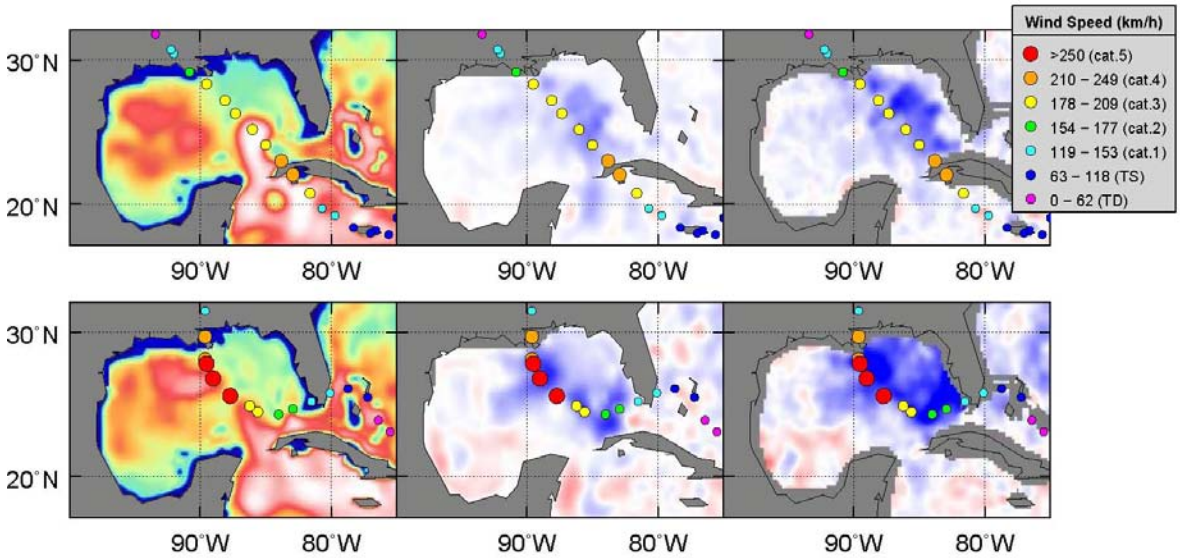

Fig. 3.12. (left) Tropical cyclone heat potential, and surface cooling given by the difference between post and pre storm values of (center) tropical cyclone heat potential and (right) sea surface temperature, for hurricanes (bottom) Katrina in 2005 and (top) Gustav in 2008. The scales are the same as in Fig. 3.11.

Sea Surface Salinity

Gregory C. Johnson[1] and John M. Lyman[1,2]

[1]NOAA/Pacific Marine Environmental Laboratory, Seattle, WA
[2]JIMAR, University of Hawaii, Honolulu, HI

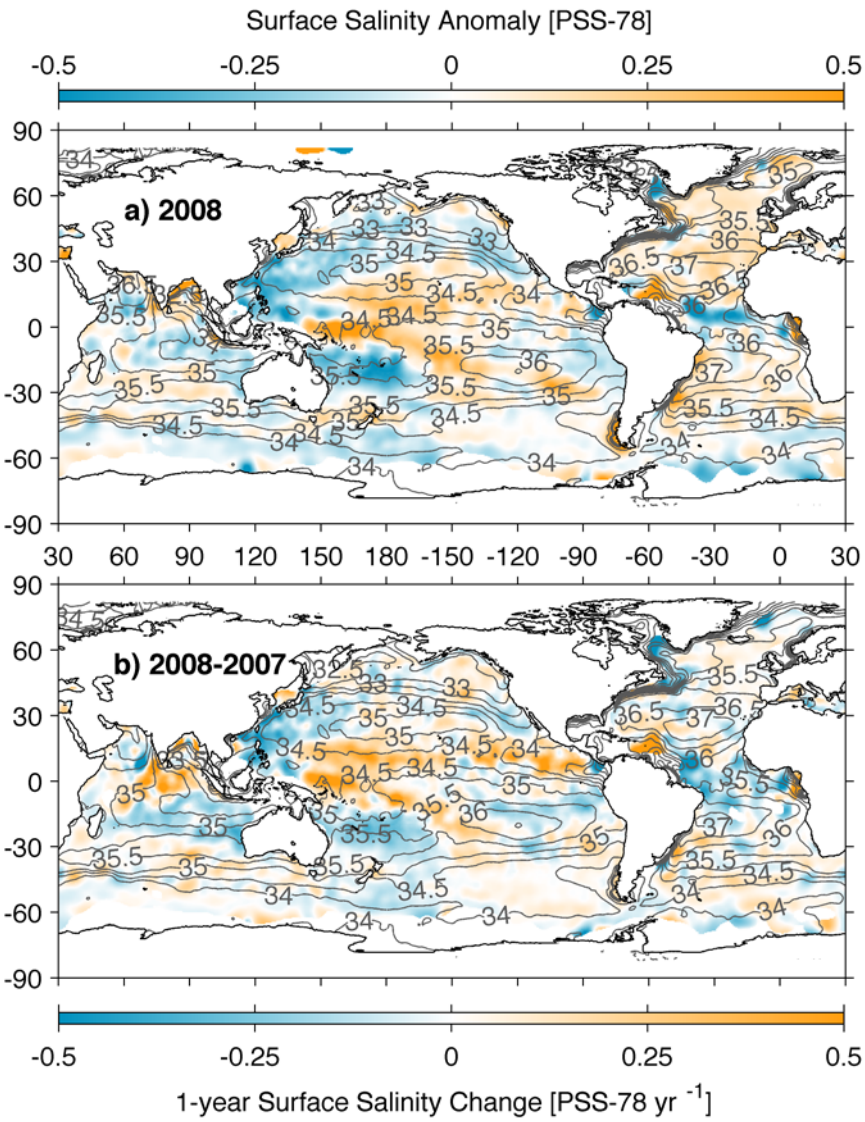

Fig. 3.13. (a) Map of the 2008 annual surface salinity anomaly estimated from Argo data [colors in PSS-78] with respect to a climatological salinity field from WOA 2001 [gray contours at 0.5 PSS-78 intervals]. (b) The difference of 2008 and 2007 surface salinity maps estimated from Argo data [colors in PSS-78 yr^{-1} to allow direct comparison with a)]. White areas are either

neutral with respect to salinity anomaly or are too data-poor to map. While salinity is often reported in practical salinity units, or PSU, it is actually a dimensionless quantity reported on the 1978 Practical Salinity Scale, or PSS-78.

Surface Current Observations

Rick Lumpkin[1], Gustavo Goni[1], and Kathleen Dohan[2]

[1] NOAA/Atlantic Oceanographic and Meteorological Laboratory, Miami, FL USA
[2] Earth and Space Research, Seattle WA USA

Surface current anomalies in 2008

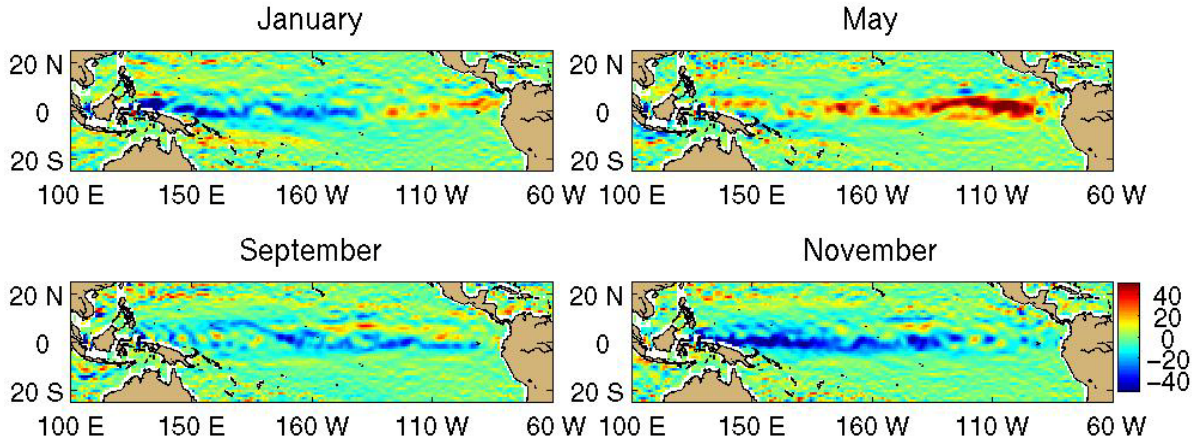

Fig. 3.14. OSCAR monthly-averaged zonal current anomalies (cm/s), positive eastward, with respect to seasonal climatology for January, May, September and November 2008.

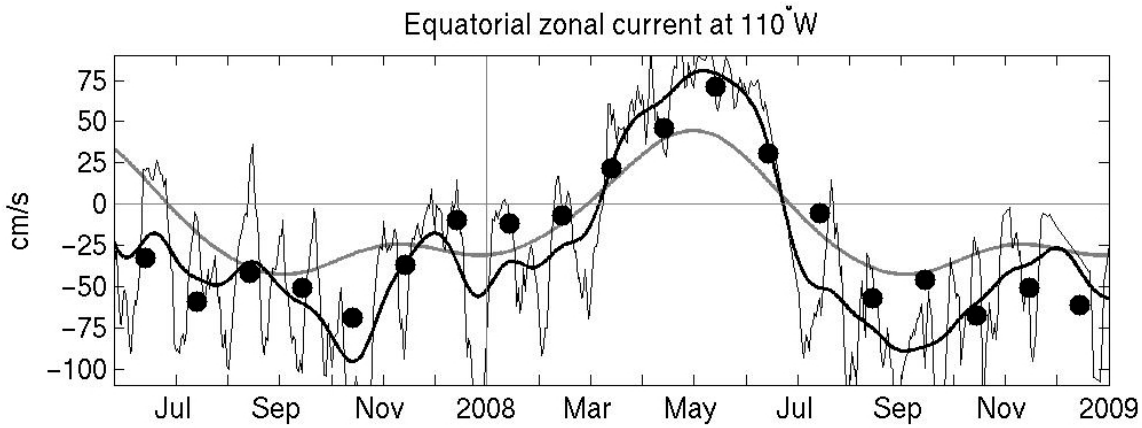

Fig. 3.15. Daily (thin black) and 15 day lowpassed (thick black) zonal currents (positive eastward) measured at the equatorial TAO mooring at 110°W, at a depth of 10m. Also shown are the mean seasonal cycle (gray) and OSCAR monthly mean zonal currents (black dots) at this location.

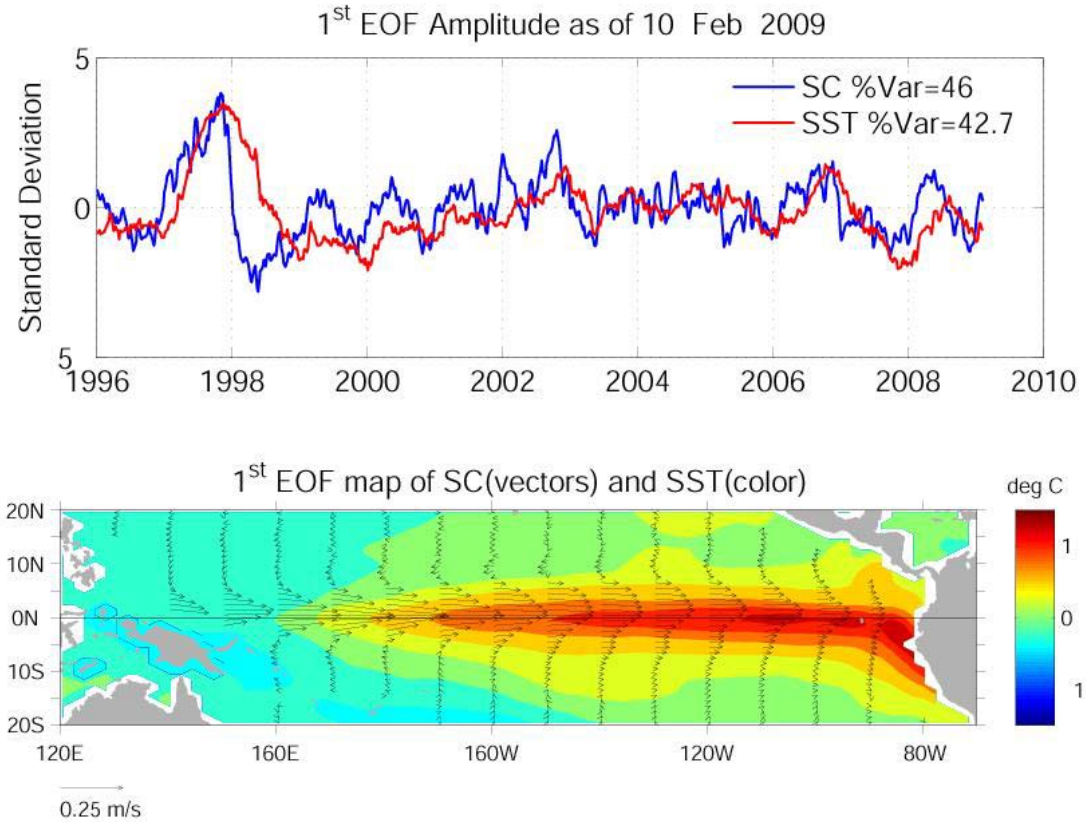

Fig 3.16. Principal empirical orthogonal functions (EOF) of surface current ("SC") and of SST anomaly variations in the Tropical Pacific. Top: amplitude time series of the EOFs normalized by their respective standard deviations. Bottom: spatial structures of the EOFs.

Long-term changes in surface currents

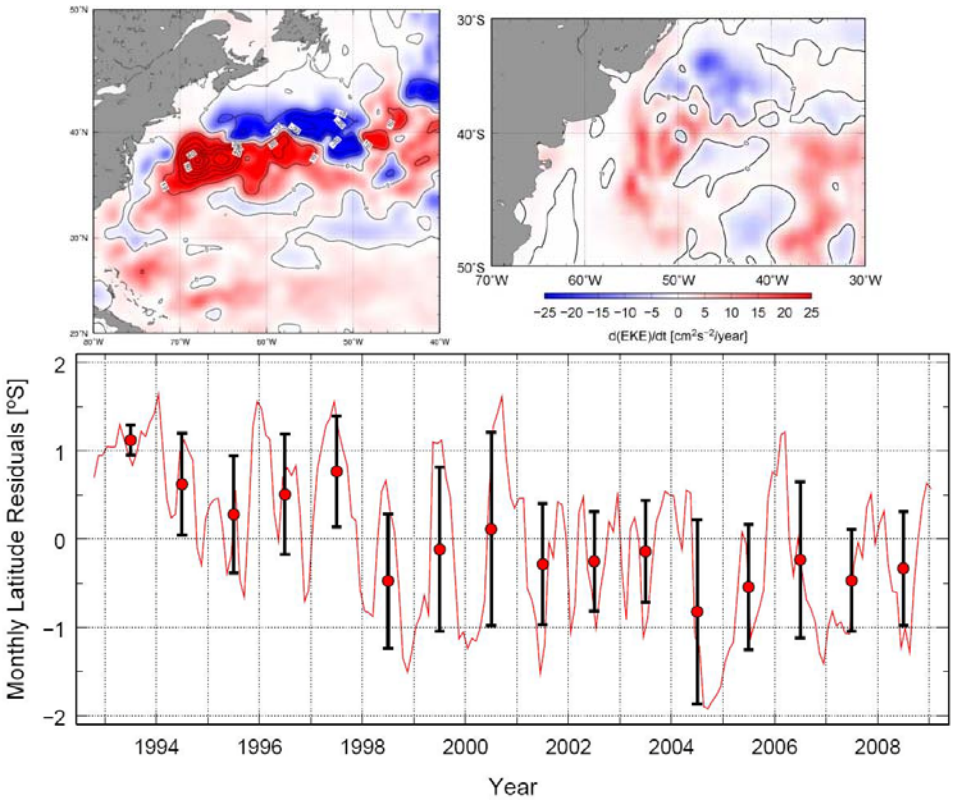

Fig 3.17. Trends in geostrophic EKE for 1993—2008 in the Gulf Stream region (top left) and the Brazil-Malvinas Confluence (top right), calculated from satellite altimetry. Bottom: location of the Brazil current separation with respect to its mean position over the period 1993—2008. Circles with bars indicate annual means and two standard deviations of the values in each calendar year.

The Meridional Overturning Circulation

M. O. Baringer[1], C. S. Meinen[1], G. C. Johnson[2], T. O. Kanzow[3], S. A. Cunningham[3], W. E. Johns[4], L. M. Beal[4], J. J-M. Hirschi[3], D. Rayner[3], H. R. Longworth[3], H. L. Bryden[3], and J. Marotzke[5]

[1] NOAA/Atlantic Oceanographic and Meteorological Laboratory, 4301 Rickenbacker Causeway, Miami, FL 33149
[2] NOAA/Pacific Marine Environmental Laboratory, Sand Point Way, Seattle, WA
[3] Ocean Observing and Climate Research Group, National Oceanography Centre, European Way, Southampton, SO17 3ZH, U.K.
[4] Division of Meteorology and Physical Oceanography, Rosenstiel School of Marine and Atmospheric Science, 4600 Rickenbacker Causeway, Miami, FL 33149
[5] Max-Planck-Institut für Meteorologie, Bundesstraße 5, 20146 Hamburg, Germany

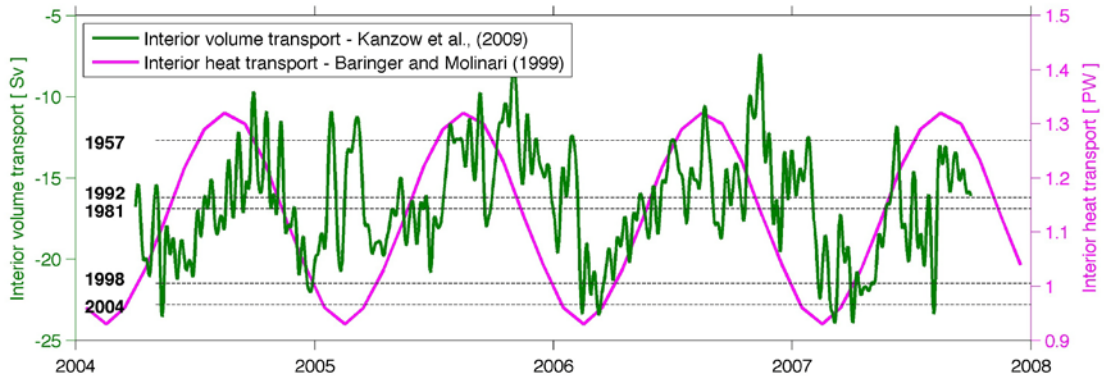

Fig. 3.18. Daily estimates of the strength of the upper 1000 meter transport (green solid) as measured by the United Kingdom's National Environmental Research Council (NERC) Rapid Climate Change Program, the National Science Foundation's Meridional Overturning and Heat transport Array, and the long-term NOAA funded Western Boundary Time Series Program. The interior volume transport estimate (accurate to 1 Sv, Cunningham et al 2007) is based on the upper ocean transport from March 2004 to October 2007 (adapted from Figure 7 from Kanzow *et al.*, 2009), with a ten day low pass filter applied to the daily transport values. Dashed black horizontal lines are the Bryden *et al.*, (2005) Upper Ocean Transport values from the 1957, 1981, 1992, 1998 and 2004 transatlantic hydrographic sections. The total heat transport (estimated error 0.2 PW) for monthly averages) is adapted from Baringer and Molinari (1999) including the mean heat transport components from Molinari et al., 1990. One PetaWatt (1PW = 10^{15}W) is

equivalent to the amount of electricity produced by one million of the largest nuclear power plants in existence today.

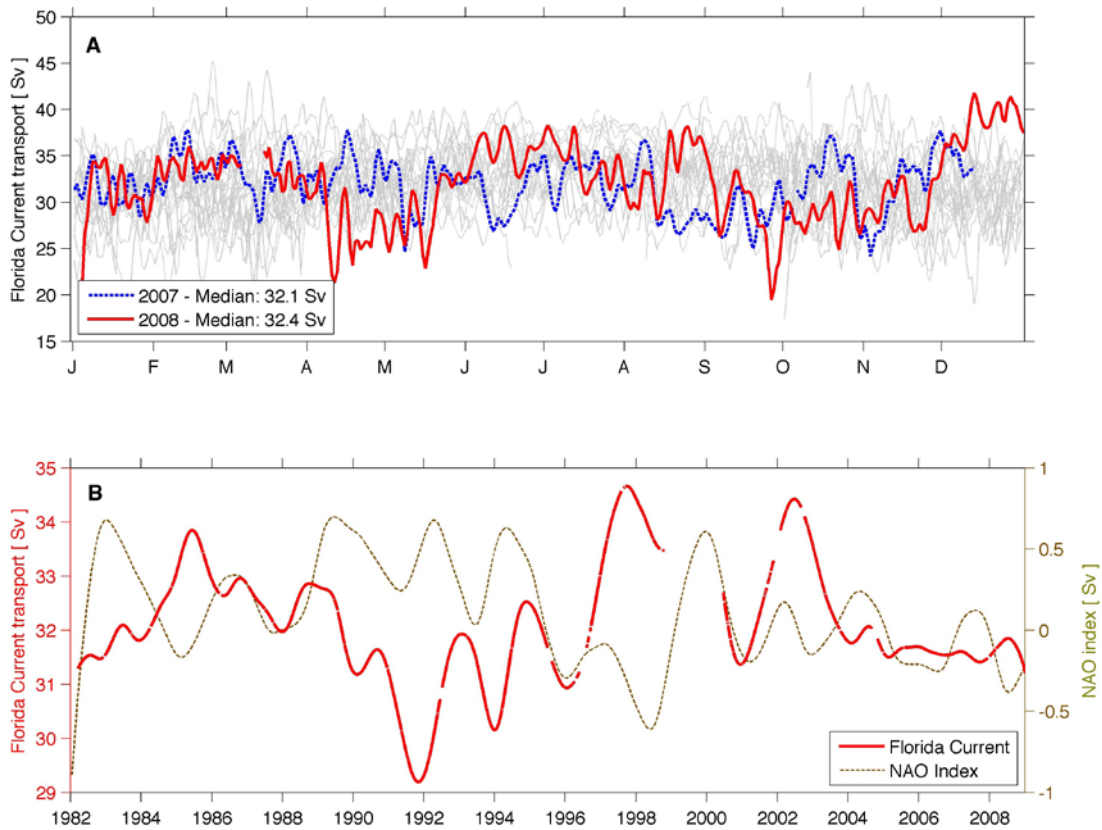

Fig. 3.19. (A, top) Daily estimates of the transport of the Florida Current for 2008 (red solid line) compared to 2007 (dashed blue line). The daily values of the Florida Current transport for other years since 1982 are shown in light grey. The median transport in 2008 increased slightly relative to 2007 and 2006, and is slightly above the long-term median for the Florida Current (32.2 Sv). (B, bottom) Two-year smoothed Florida Current transport (red) and NAO index (dashed orange). The daily Florida Current transport values are accurate to 1.1-1.7 Sv (Meinen *et al.*, 2009) and the smoothed transport to 0.25 Sv (a priori estimate using the observed 3-10 day independent time scale).

Sea Level Variations, 2008 Annual Assessment

Mark A. Merrifield[1], R. S. Nerem[2], Gary T. Mitchum[3], Laury Miller[4], Eric Leuliette[4], Stephen Gill[5], Philip L. Woodworth[6]

[1] University of Hawaii at Manoa, Honolulu, Hawaii
[2] University of Colorado, Boulder, Colorado
[3] University of South Florida, College of Maine Science, St. Petersburg, Florida
[4] NOAA/NESDIS, Laboratory for Satellite Altimetry, Silver Spring, Maryland
[5] NOAA/NOS Center for Operational Oceanographic Products and Services, Silver Spring, Maryland
[6] Proudman Oceanographic Laboratory, Liverpool, United Kingdom

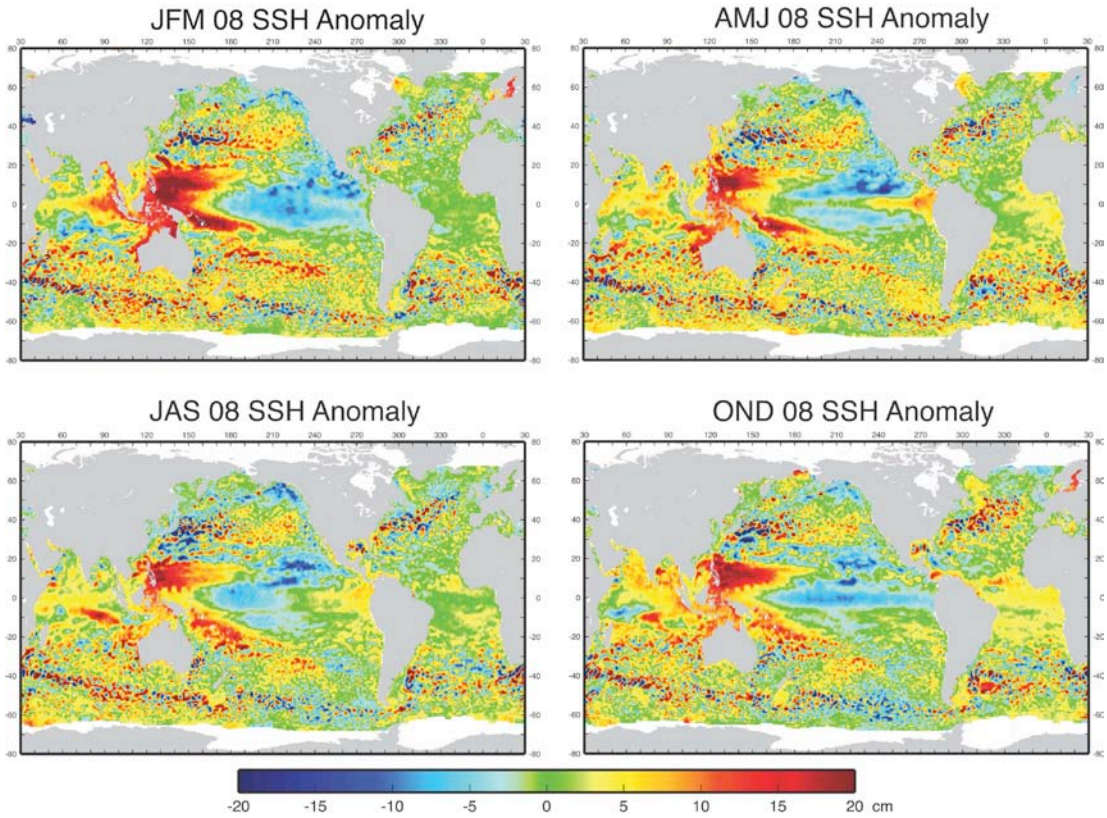

Fig. 3.20. Seasonal SSH anomalies for 2008 relative to the 1993-2007 baseline average are obtained using the multimission gridded sea surface height altimeter product produced by Ssalto/Duacs and distributed by Aviso, with support from CNES (www.aviso.oceanobs.com).

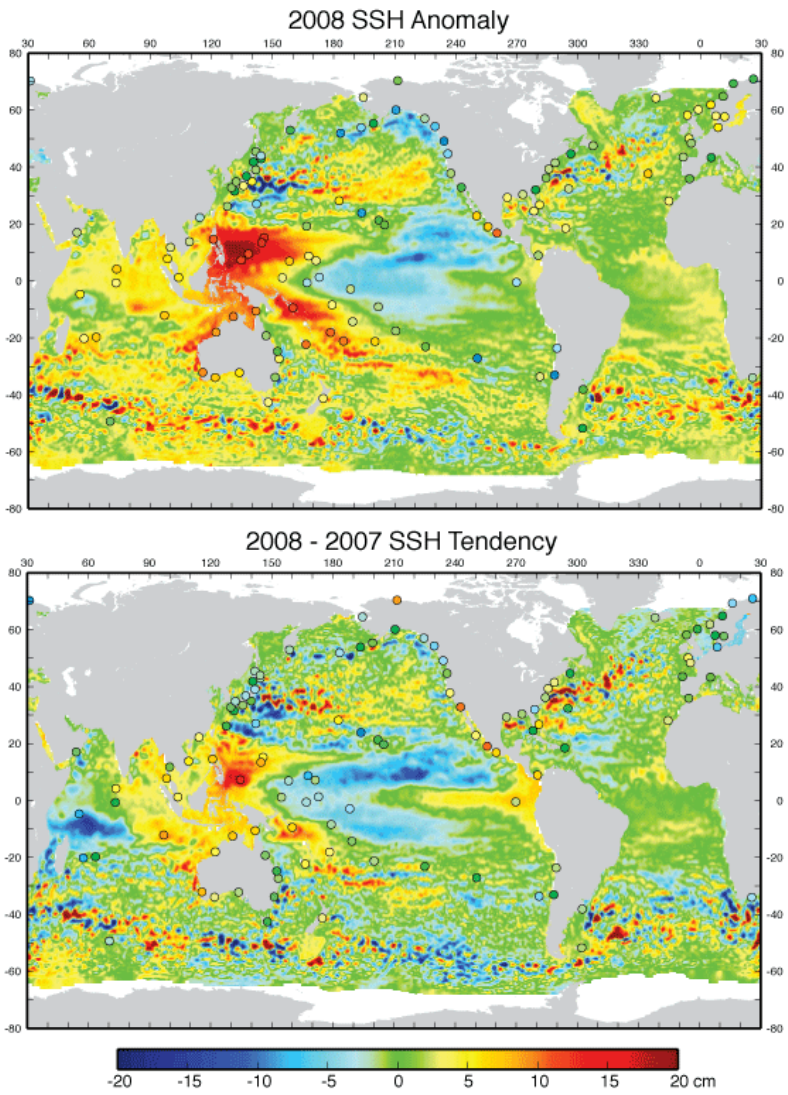

Fig. 3.21. Top: The 2008 SSH anomaly (Ssalto/Duacs product) from the 1993-2007 baseline is compared to the 2008 anomaly computed for tide gauge data (dots) obtained from the University of Hawaii Sea Level Center (http://uhslc.soest.hawaii.edu/). Bottom: The difference between 2008 and 2007 annual means.

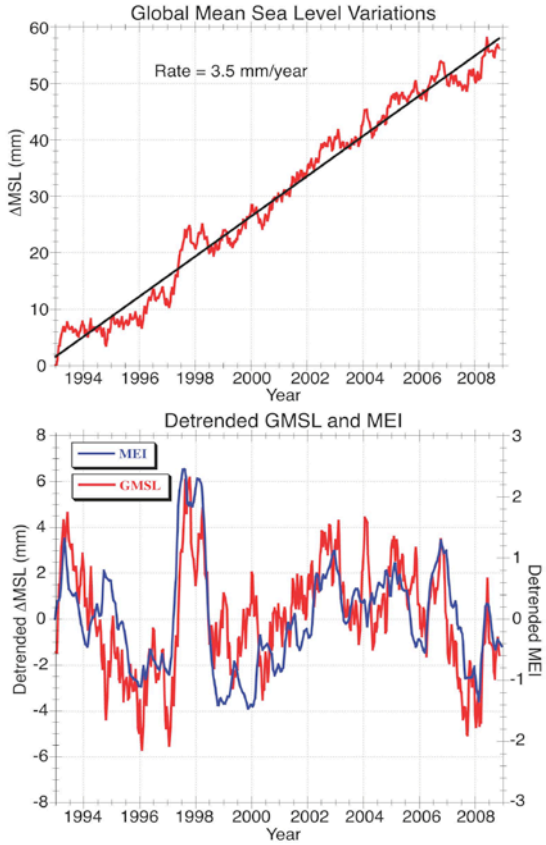

Fig. 3.22. Top: Monthly GMSL (seasonal cycle removed) relative to a linear trend of 3.5 mm yr^{-1}. Bottom: Monthly GMSL (linear trend removed, red) versus the Multivariate ENSO Index (MEI, blue). SSH data provided by the NASA Physical Oceanography Distributed Active Archive Center (PO.DAAC) at the Jet Propulsion Laboratory/California Institute of Technology (http://podaac.jpl.nasa.gov/).

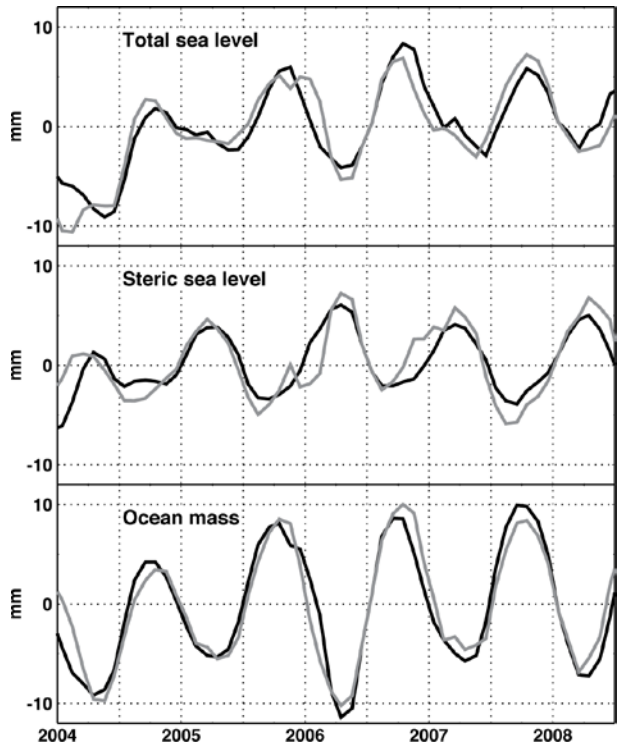

Fig. 3.23. Time series of GMSL or Total sea level, is compared with the two principal components of sea level change, upper-ocean steric change from Argo measurements and mass change from GRACE measurements (*Leuliette and Miller*, 2009)_. In this figure, black lines show the observed values and gray lines the inferred values from the complementary observations (e.g., the inferred steric sea level is obtained from observed total sea level – observed ocean mass).

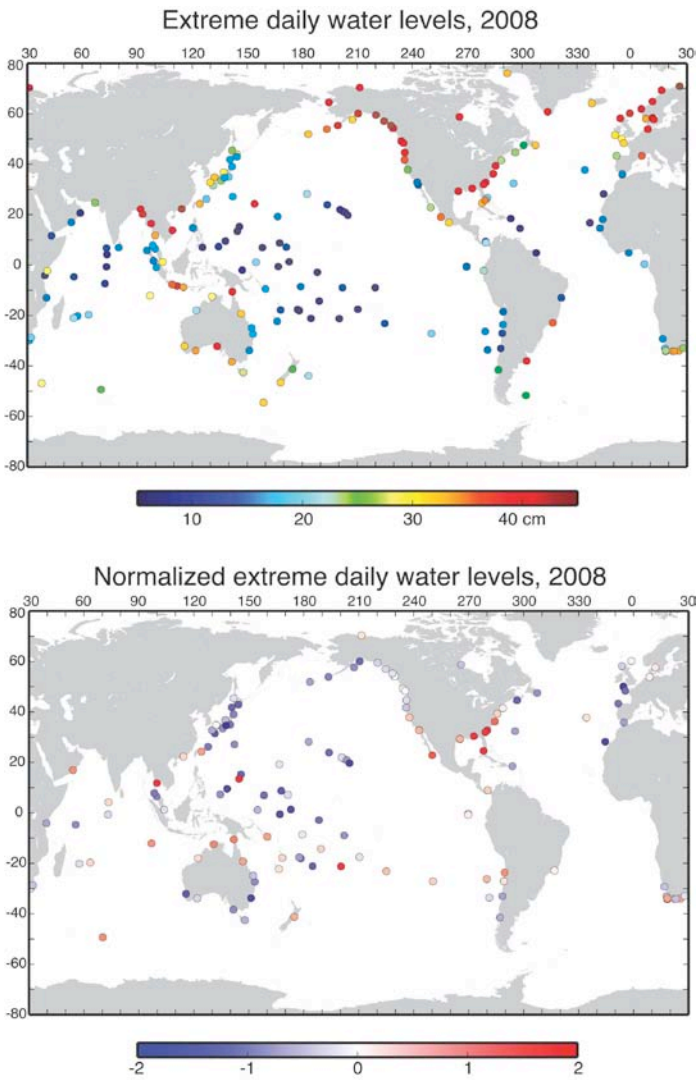

Fig. 3.24. Top: Extreme sea level variability is characterized using the average of the top 2% mean daily sea levels during 2008 relative to the annual mean at each station. Bottom: The extreme values are normalized by subtracting the mean and dividing by the standard deviation of past year extreme values for stations with at least 15 year record lengths.

The Global Ocean Carbon Cycle

Christopher L. Sabine[1], Richard A. Feely[1], Rik Wanninkhof[2], and Taro Takahashi[3]

[1] NOAA/OAR Pacific Marine Environmental Laboratory, Seattle, WA
[2] NOAA/OAR Atlantic Oceanographic and Meteorological Laboratory, Ocean Chemistry Division, Miami, FL
[3] Lamont-Doherty Earth Observatory, Columbia University, Palisades, New York

1) Air-Sea Carbon Dioxide Fluxes

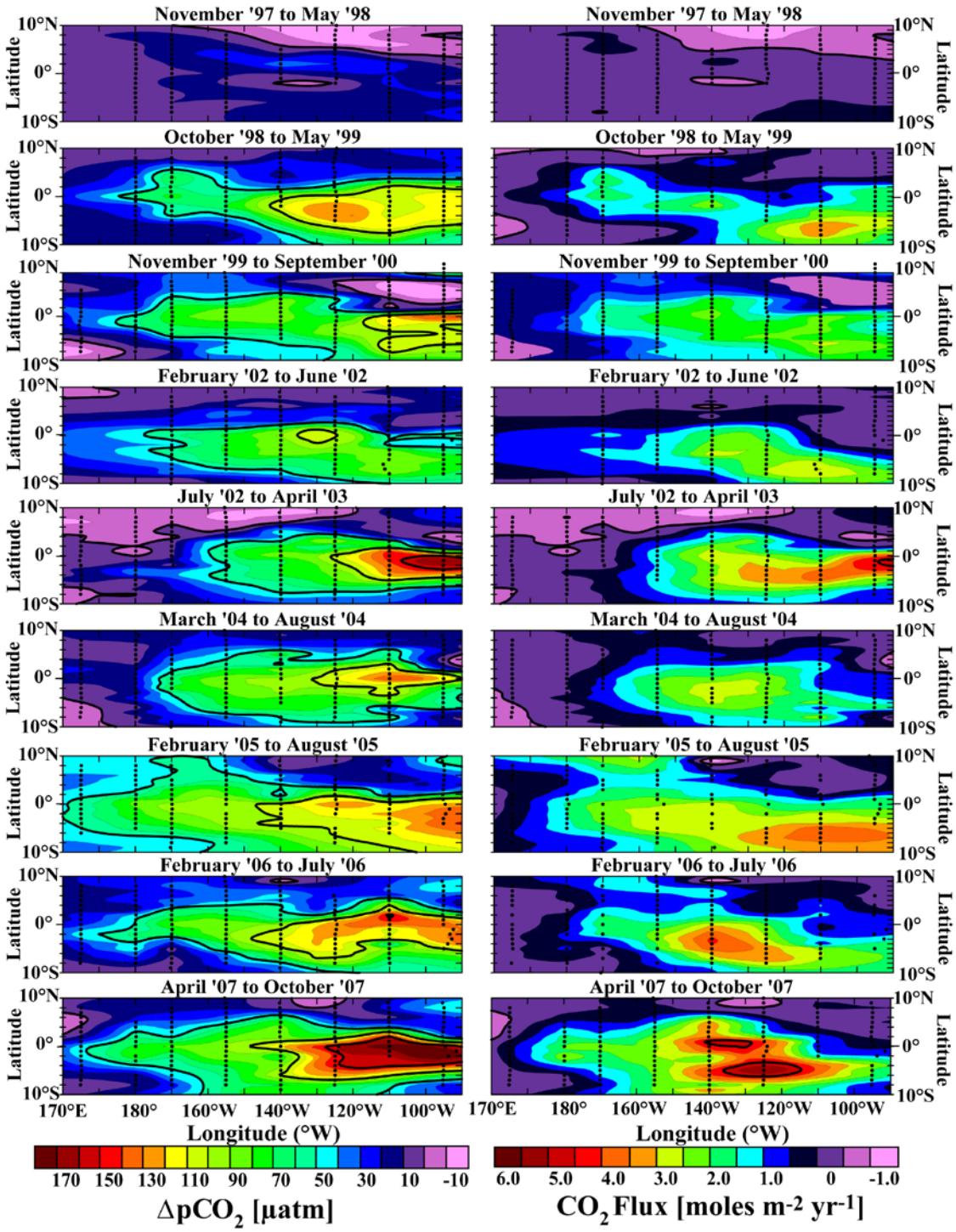

Fig. 3.25. Plots of sea-air pCO_2 difference and air-sea CO_2 flux in the Equatorial Pacific between 1997 and 2007 based on underway CO_2 measurements collected on the TAO service cruises. The nominal cruise track lines are shown in black. A complete survey of the region is completed approximately every six months. The black and dark purple colors indicate areas where the atmosphere and seawater pCO_2 values are nearly balanced. The pink colors indicate areas of ocean uptake of CO_2 and the blue to red colors indicate areas of ocean CO_2 out-gassing.

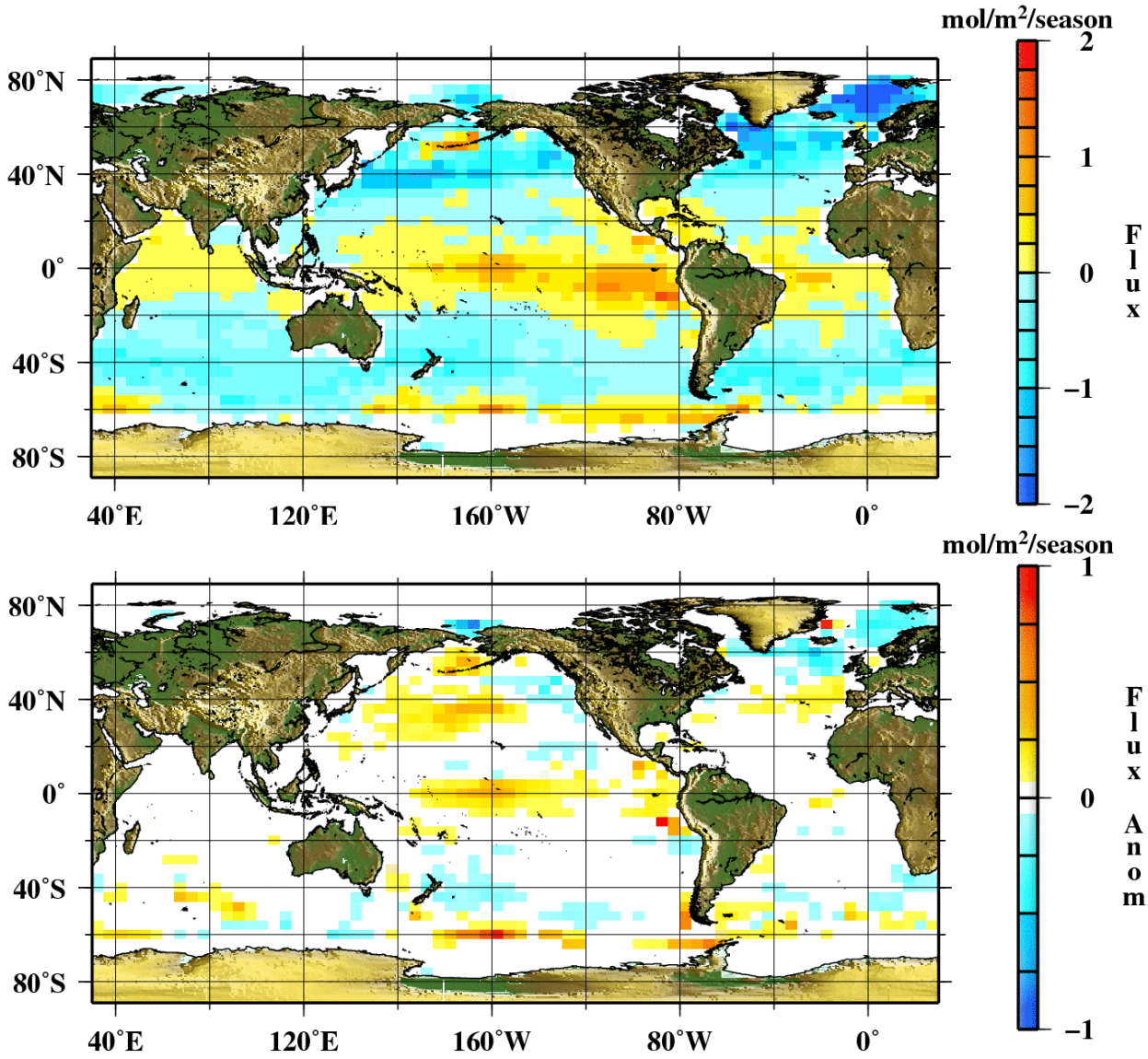

Fig. 3.26 . chapter3f1 **Fig. 3.26.** Maps of (a, upper panel) net air-sea CO_2 fluxes and (b, lower panel) air-sea CO_2 flux anomaly for September-December 2007. Coastal pixels and those with ice cover are masked in white. Negative fluxes represent uptake of CO_2 by the ocean. Output and graphic provided by J. Trinanes.

2) Subsurface Carbon Inventory

Table 1. estimates of ocean column inventory changes in anthropogenic carbon (mol C m^{-2} yr^{-1}) over the last decade.

	Atlantic (25°W) 1993-2005	Pacific (152°W) 1991-2006	Indian (90°E) 1995-2007
Northern Hemisphere	0.63	0.25	0.63
Southern Hemisphere	0.75	0.41	0.83

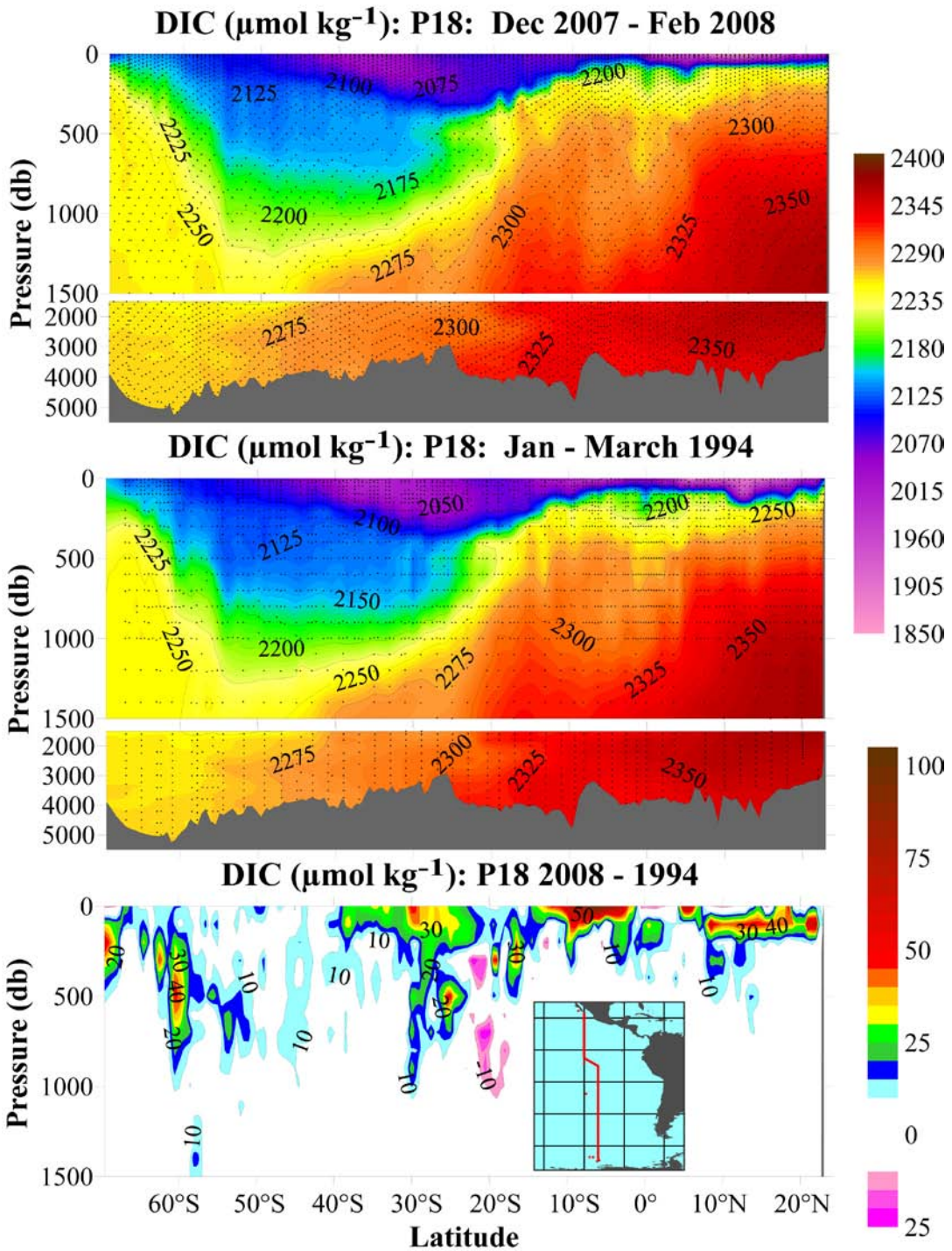

Fig. 3.27. Sections of dissolved inorganic carbon (µmol kg^{-1}) nominally along 105°W in 2008 (top) and 1994 (middle). The bottom section shows the DIC change between the two cruises (2008-1994). Black dots show sample locations. Inset map shows cruise track in red.

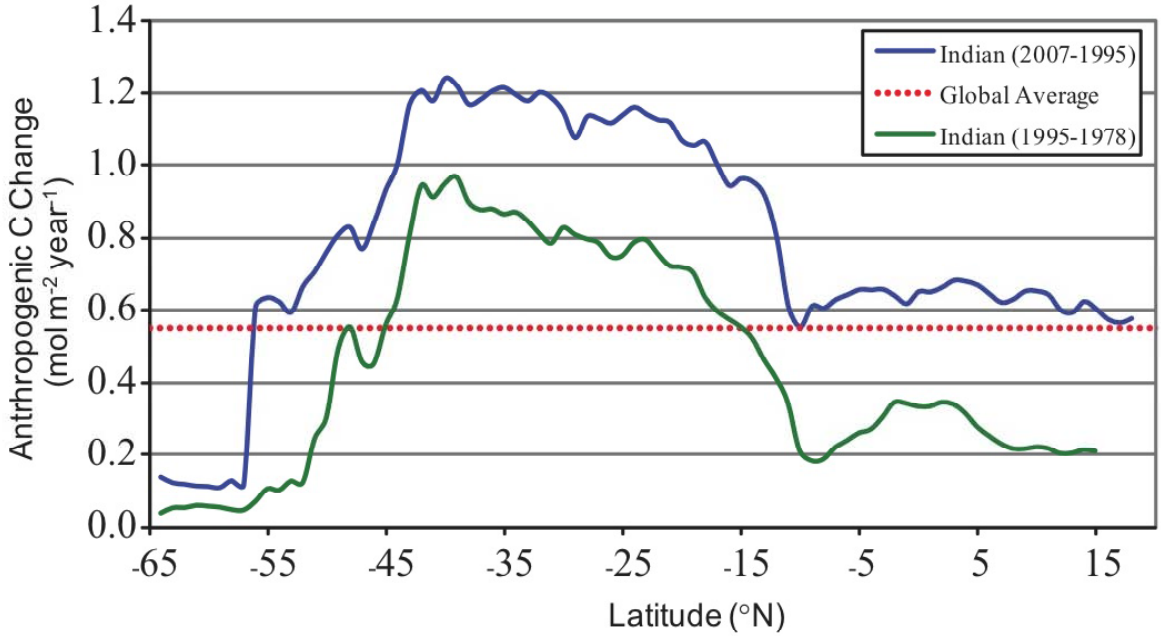

Fig. 3.28. Column Inventory changes as a function of latitude along ~90°E in the eastern Indian Ocean. The blue line is the average annual change between 2007 and 1995. The green line is the average annual change between 1995 and 1978. The red dotted line is the global average annual uptake of anthropogenic CO_2 divided by the surface area of the ocean.

New Evidence for Ocean Acidification in Coastal Waters of North America

(Sidebar)

Richard A. Feely[1] and Andrew G. Dickson[2]

[1]NOAA/OAR Pacific Marine Environmental Laboratory, Seattle, WA
[2]Scripps Institution of Oceanography, University of California, San Diego, La Jolla, CA

.

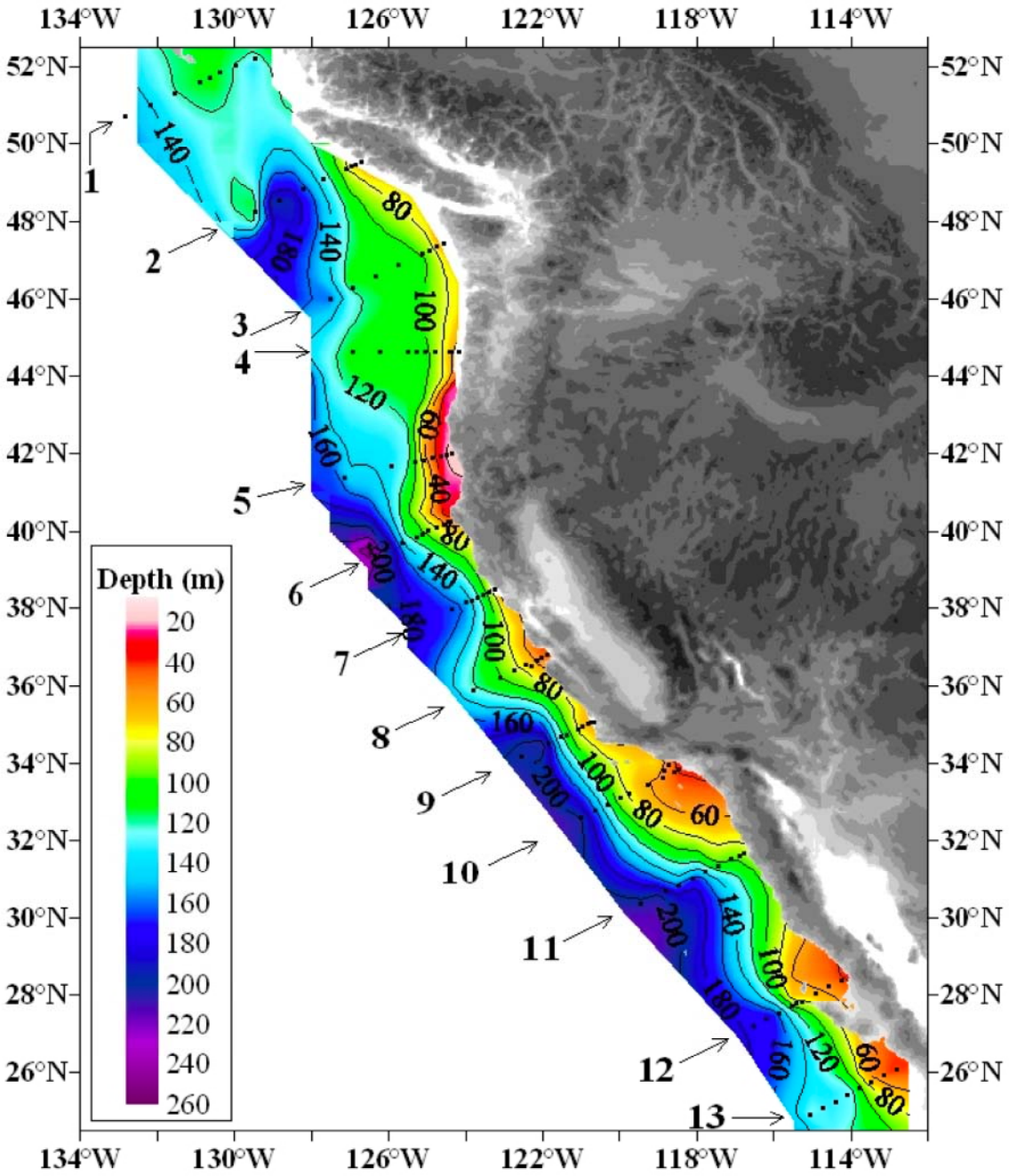

Fig. 3.29. (after Feely et al. 2008). Distribution of the depths of "ocean acidified" undersaturated water (aragonite saturation < 1.0; pH < 7.75) on the continental shelf of western North America from Queen Charlotte Sound, Canada, to San Gregorio Baja California Sur, Mexico. On transect line 5, the corrosive water reaches all the way to the surface in the inshore waters near the coast. The black dots represent station locations.

Global Ocean Phytoplankton

Michael J. Behrenfeld[1], David A. Siegel[2], Robert T. O'Malley[1], Stephane Maritorena[2]

[1] Oregon State University, Corvallis, Oregon
[2] University of California at Santa Barbara, Santa Barbara, California

Figure 1

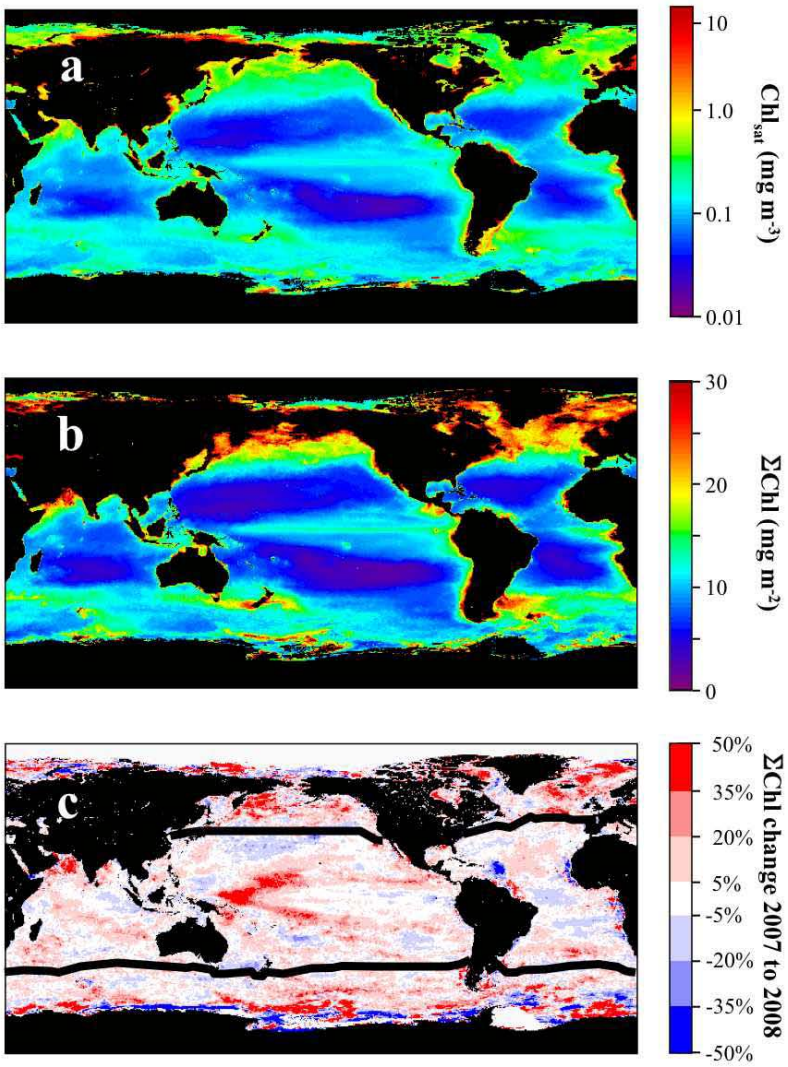

Fig. 3.30. (a) Average MODIS-Aqua surface chlorophyll concentration (Chl_{sat}) for 2008. (b) Average MODIS-Aqua photic zone chlorophyll content (ΣChl) for 2008. (c) Percentage change in ΣChl from 2007 to 2008. Heavy black lines demark permanently stratified oceans (2007 average SST >15°C) from higher latitude regions (2007 average SST < 15°C). Because data were only available through day 320 of 2008 at the time of our analysis, here and in the main text annual values are for Julian dates 321 of a given year to 320 of the following year (e.g., the 2008 period = Julian day 321, 2007 to Julian day 320, 2008). Photic zone chlorophyll content calculated following Behrenfeld et al. (2006).

Figure 2

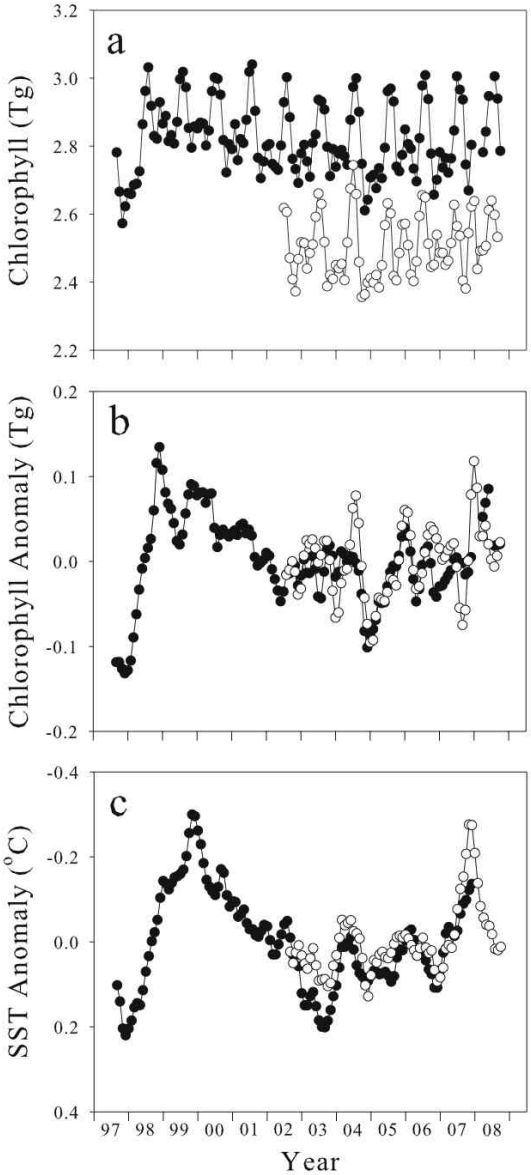

Fig. 3.31. (a) Monthly photic zone chlorophyll concentrations (= average ΣChl times area) for the permanently stratified oceans (SST >15°C; Fig. 3.30). Solid symbols = SeaWiFS data. Open symbols = MODIS-Aqua data. (b) Monthly anomalies in stratified ocean photic zone chlorophyll for SeaWiFS (solid symbols) and MODIS-Aqua (open symbols). Anomalies represent the difference between photic zone chlorophyll for a given month and the average value for that month for a given sensor record. (c) Monthly anomalies in mean SST for the stratified oceans based on AVHRR quality 5 - 8 data (solid symbols) and MODIS 4 um data (open symbols).

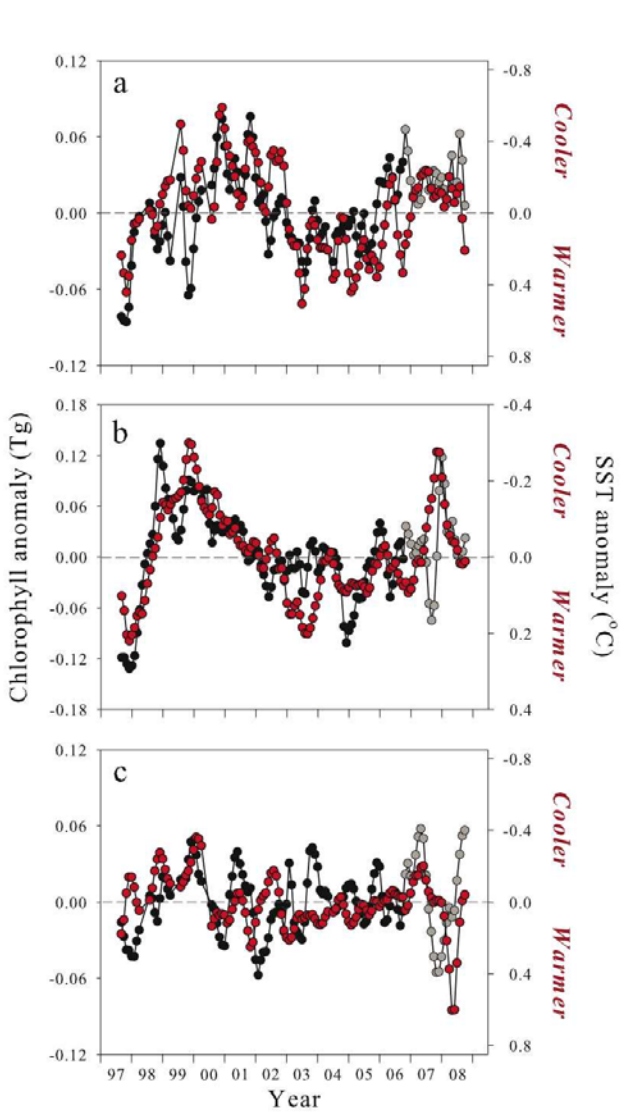

Fig. 3.32. Comparison of monthly anomalies in photic zone chlorophyll (black and gray symbols, left axis) and SST (red symbols, right axis). (a) Northern waters with 2007 average SST < 15°C. (b) Permanently stratified waters with 2007 average SST > 15°C. (c) Southern waters with 2007 average SST < 15°C. (a-c) Solid black symbols = SeaWiFS data. Gray symbols = MODIS-Aqua data. MODIS-Aqua data are spliced into the SeaWiFS record beginning on Julian day 321, 2006, to be consistent with Fig. 3.30. Horizontal dashed line in each panel corresponds to monthly climatological average values. Note, left axes increase from bottom to top, while right axes decrease from bottom to top.